Chemistry of Metals and Alloys

Chem. Met. Alloys 2 (2009) 115-122
Ivan Franko National University of Lviv
www.chemetal-journal.org

Crystal structure of the compound Pr_4Ge_7

Oleh SHCHERBAN[1], Igor SAVYSYUK[1], Nataliya SEMUSO[1]*, Roman GLADYSHEVSKII[1], Karin CENZUAL[2]

[1] *Department of Inorganic Chemistry, Ivan Franko National University of Lviv, Kyryla i Mefodiya St. 6, UA-79005 Lviv, Ukraine*
[2] *Département de Chimie Minérale, Analytique et Appliquée, Université de Genève, Quai Ernest Ansermet 30, CH-1211 Geneva, Switzerland*
* *Corresponding author. Tel.: +38 032 2394163; e-mail: nakonechna_n@franko.lviv.ua*

Received May 1, 2009; accepted June 30, 2009; available on-line November 16, 2009

The structure of the binary germanide Pr_4Ge_7 has been determined by single-crystal X-ray diffraction on a twinned crystal. It is an ordered vacancy derivative of the α-$ThSi_2$ type, Pearson symbol *oS*44, space group *C*222$_1$, *a* = 6.007(2), *b* = 13.987(4), *c* = 12.009(4) Å, isotypic to the structure reported earlier for Nd_4Ge_7. The cell parameters of seven other praseodymium germanides observed in samples annealed at 873 K were refined from powder X-ray diffraction data.

Germanide / Praseodymium / Single-crystal X-ray diffraction / Crystal structure / Vacancy derivative

Introduction

According to the phase diagram [1-3], eight binary compounds form in the Pr-Ge system: Pr_3Ge, Pr_5Ge_3, Pr_4Ge_3, Pr_5Ge_4, PrGe (CrB), PrGe (FeB), $PrGe_{2-x}$, and $PrGe_2$. The crystal structures of the compounds containing less than 60% Ge are well established, however, the literature data gathered in Table 1 reveal a more complex situation in the Ge-rich part of the system. The stoichiometric compound $PrGe_2$ mentioned above is probably identical with $PrGe_{1.91}$ [13], which crystallizes with a structure related to the $TbGe_2$ type.

According to Eremenko *et al.* [2] the non-stoichiometric digermanide $PrGe_{2-x}$ exists in the range 60.8-62.7 at.% Ge and undergoes a transition at 548-615ºC from a tetragonal high-temperature phase with an α-$ThSi_2$-type structure to an orthorhombic room-temperature phase with an α-$GdSi_2$-type structure. Schobinger-Papamantellos *et al.* [9] observed a tetragonal phase with significant change of cell parameters at compositions near $PrGe_{1.7}$. The superstructure observed in a sample $PrGe_{1.60}$ was refined in space group *Fdd*2. Boutarek *et al.* [11] reported the coexistence of two tetragonal phases with different *c*/*a* ratios, called Q_1 and Q_2, in a sample $PrGe_{1.74}$. The former was found to be single phase at $PrGe_{1.58}$, the latter at $PrGe_{1.8}$. In a later work [10] a sample of composition $PrGe_{1.6}$ contained a majority phase, identified as Q_1, with partly ordered vacancies, which was refined in the orthorhombic Y_3Ge_5 structure type [14], and a minority α-$ThSi_2$-type phase Q_2 with disordered vacancies. Venturini *et al.* [12,15] carried out a systematic study of non-stoichiometric digermanides of the rare earths and several structural models with ordered Ge vacancies derived from the α-$ThSi_2$ type were proposed, among which the orthorhombic structure type Nd_4Ge_7.

Here we present data for binary Pr-Ge compounds obtained during investigations of the Pr-Ag-Ge and Pr-Al-Ge ternary systems [16,17].

Experimental

Binary Pr-Ge samples were prepared from high-purity components (Pr > 99.9 and Ge > 99.999 wt.%) by arc melting under an argon atmosphere; the weight losses were less than 2 wt.%. The alloys were consecutively annealed in evacuated silica tubes at 873 K for 30 days and quenched into cold water.

Preliminary phase analysis was carried out based on diffraction patterns recorded with a Debye-Scherrer camera (diameter 53.7 mm) using Cr *K* radiation. The unit cell parameters were refined on X-ray diffraction data from polycrystalline samples, recorded on a diffractometer DRON-2.0 (Fe *K*α radiation, λ = 1.93735 Å, internal silicon standard). The programs POWDER CELL [18] and LATCON [19] were used for the calculations.

Single crystals of Pr_4Ge_7 were selected from a ternary alloy of nominal composition $Pr_{33.3}Al_{6.7}Ge_{60}$.

6382 reflections indexed on a pseudotetragonal cell 12.01×12.01×13.99 Å were collected on an Enraf-Nonius CAD-4 automatic diffractometer. Refinement in an α-$ThSi_2$ structure type subcell gave ~1/8 vacancies on the Ge site. No satisfactory model could be refined for the cell mentioned above. A more detailed analysis led to the conclusion that the true unit cell is smaller (6.007(2)×12.009(4)×13.987(4) Å). Fig. 1 shows that the diffraction pattern can be explained considering twinning where the unit cell vectors of the crystallites correlate via the matrix:

$$\begin{vmatrix} 0 & 1 & 0 \\ 1 & 0 & 0 \\ 0 & 0 & -1 \end{vmatrix}.$$

The study of possible group-subgroup relationships starting from the α-$ThSi_2$ type (space group $I4_1/amd$) led to a model in space group $C222_1$ for the new unit cell (Table 2). This model was identical with the structure reported for Nd_4Ge_7 [12]. The twinning corresponds to ordering of vacancies on the Ge sites in two mutually perpendicular directions with respect to the small tetragonal cell of the parent structure. For the refinement, equal contributions of both twins were considered. The program used to refine the structure was from SHELX-97 [20]. Structure data and details concerning the data collection and structure refinement are given in Table 3.

Table 1 Crystallographic parameters of binary compounds in the Pr-Ge system (selected literature data from [4] and results of this work).

Ge content (at.%)	Compound	Structure type	Space group	Pearson symbol	Cell parameters (Å)			Reference
					a	*b*	*c*	
25.0	Pr_3Ge	Ti_3P	$P4_2/n$	*tP*32	12.422	–	6.118	[5]
					12.418(5)	–	6.133(2)	[6]
37.5	Pr_5Ge_3	Mn_5Si_3	$P6_3/mcm$	*hP*16	8.84	–	6.63	[2]
					8.801(2)	–	6.659(3)	this work
42.7	Pr_4Ge_3	Th_3P_4	$I\bar{4}3d$	*cI*28	9.32	–	–	[2]
					9.1460(6)	–	–	this work
44.4	Pr_5Ge_4	Sm_5Ge_4	*Pnma*	*oP*36	7.9141	15.1829	8.0060	[7]
					7.945(7)	15.199(8)	7.951(7)	this work
50.0	PrGe	CrB	*Cmcm*	*oS*8	4.480	11.092	4.054	[8]
					4.486(4)	11.09(1)	4.066(9)	this work
50.0	PrGe	FeB	*Pnma*	*oP*8	8.294	4.053	5.982	[8]
					8.301(4)	4.053(2)	5.962(4)	this work
61.5	β-$PrGe_{1.6}$	α-$ThSi_2$	$I4_1/amd$	*tI*12	4.43	–	14.00	[2]
61.5	α-$PrGe_{1.6}$	α-$GdSi_2$	*Imma*	*oI*12	4.27	4.18	14.22	[2]
61.5	$PrGe_{1.60}$ (60 K)	Y_3Ge_5	*Fdd*2	*oF*64	5.9193	17.7582	14.128	[9]
61.5	$PrGe_{1.60}$ (Q_1)	Y_3Ge_5	*Fdd*2	*oF*64	5.928	17.785	14.07	[10]
61.5	$PrGe_{1.60}$ (Q_2)	α-$ThSi_2$	$I4_1/amd$	*tI*12	4.228	–	14.00	[10]
61.2	$PrGe_{1.58}$ (Q_1)				4.201	–	14.101	[11]
60.0-61.8	$PrGe_{1.50\text{-}1.62}$	α-$ThSi_2$	$I4_1/amd$	*tI*12	4.1980(1)-4.2037(6)	–	14.131(3)-14.093(5)	this work
62.1	ε'-$PrGe_{1.64}$	*orthorhombic*			5.929	5.930	14.139	[12]
62.5	α'-Pr_3Ge_5	Y_3Ge_5	*Fdd*2	*oF*64	5.937	17.817	14.111	[12]
63.6	β'-Pr_4Ge_7	Nd_4Ge_7	$C222_1$	*oS*44	5.992	14.003	12.002	[12]
					6.007(2)	13.987(4)	12.009(4)	this work
63.9	γ'-$PrGe_{1.77}$	*orthorhombic*			6.024	6.021	13.966	[12]
63.9	δ'-$PrGe_{1.77}$	*orthorhombic*			6.018	6.022	13.978	[12]
64.3	$PrGe_{1.8}$ (Q_2)				4.248	–	14.001	[11]
62.7-64.4	$PrGe_{1.68\text{-}1.81}$	α-$ThSi_2$	$I4_1/amd$	*tI*12	4.243(1)-4.260(1)	–	14.010(6)-13.965(2)	this work
65.6	$PrGe_{1.91}$	$PrGe_{1.91}$	*Cmcm*	*oS*36	4.2721(6)	30.673(4)	4.1433(6)	[13]

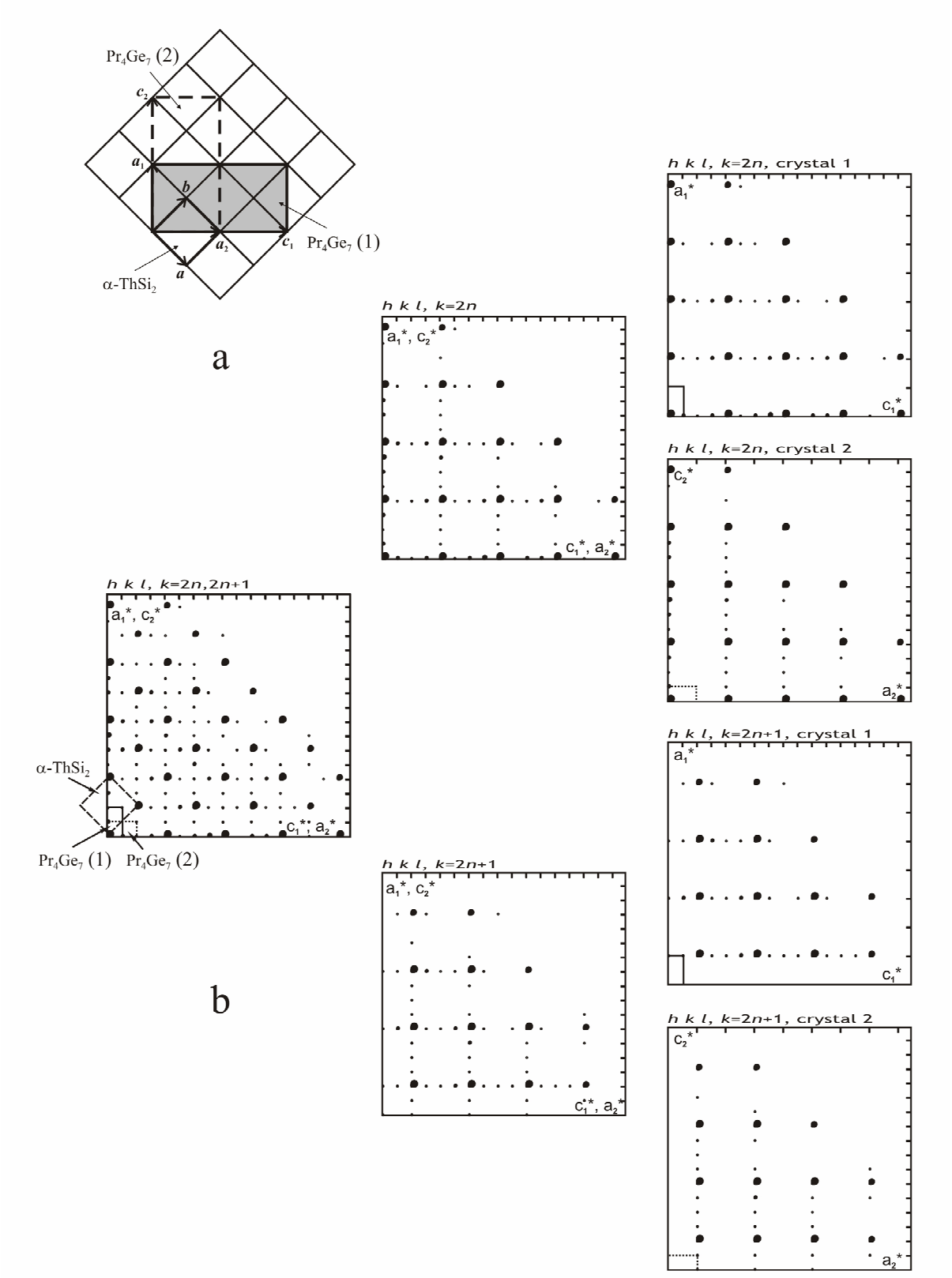

Fig. 1 Relative orientation of the twins in the crystal used for the refinement of the structure of Pr_4Ge_7 (a) and decomposition of the diffraction pattern into contributions from crystal 1 and crystal 2 (b).

Table 2 Group-subgroup relationship between the structures of α-$ThSi_2$ (**I**) and Pr_4Ge_7 (**V**) (site Ge(5) is vacant).

Model	**I**	**II**	**III**	**IV**	**V**
Transformation matrix		1 0 0 0 1 0 0 0 1	1 1 0 −1 1 0 0 0 1	−1 1 0 0 0 1 1 1 0	−1 1 0 0 0 1 2 2 0
Space group	$I4_1/amd$	$I4_122$	$F222$	$C222$	$C222_1$
Cell parameters (Å)	a_I=4.260 (b_I=a_I=4.260) c_I=13.965	a_{II}=a_I=4.260 (b_{II}=a_I=4.260) c_{II}=c_I=13.965	a_{III}=$\sqrt{2}$ a_I=6.025 b_{III}=$\sqrt{2}$ a_I=6.025 c_{III}=c_I=13.965	a_{IV}=$\sqrt{2}$ a_I=6.025 b_{IV}=c_I=13.965 c_{IV}=$\sqrt{2}$ a_I=6.025	a_V=$\sqrt{2}$ a_I=6.025 b_V=c_I=13.965 c_V=2$\sqrt{2}$ a_I=12.050
Site, Wyckoff position, atom coordinates	Pr 4*a* 0 ¾ ⅛	Pr 4*a* 0 0 0	Pr(1) 4*c* ¼ ¼ ¼	Pr(1) 4*k* ¼ ¼ 0.2500	Pr(1) 8*c* 0.2500 0.2500 0.3750
			Pr(2) 4*a* 0 0 0	Pr(2) 2*c* ½ 0 ½	Pr(2) 4*b* 0 0.5000 ¼
				Pr(3) 2*a* 0 0 0	Pr(3) 4*a* 0.0000 0 0
	Ge 8*e* 0 ¼ 0.2915	Ge 8*c* 0 0 0.4165	Ge(1) 8*h* ¼ ¼ 0.6665	Ge(1) 8*l* 0.2500 0.6665 0.2500	Ge(2) 8*c* 0.2500 0.1665 0.1250
					Ge(3) 8*c* 0.2500 0.3335 0.1250
			Ge(2) 8*g* 0 0 0.4165	Ge(2) 4*g* 0 0.4165 0	Ge(1) 8*c* 0.0000 0.4165 0.0000
				Ge(3) 4*h* 0 0.0835 ½	Ge(4) 4*b* 0 0.0835 ¼
					Ge(5) 4*b* 0 0.9165 ¼

Results and discussion

Crystallographic data for the binary Pr-Ge phases as determined in this work are included in Table 1. Nine germanides, Pr_3Ge, Pr_5Ge_3, Pr_4Ge_3, Pr_5Ge_4, PrGe (CrB), PrGe (FeB), $PrGe_{2-x}$ (Q_1), $PrGe_{2-x}$ (Q_2), and $PrGe_{1.91}$, were observed in the binary alloys annealed at 873 K. The cell parameters and homogeneity ranges of the non-stoichiometric digermanides $PrGe_{2-x}$ Q_2 ($0.19 < x < 0.32$, 64.4-62.7 at.% Ge) and Q_1 ($0.38 < x < 0.50$, 61.8-60.0 at.% Ge), shown in Fig. 2, are close to those reported in [11].

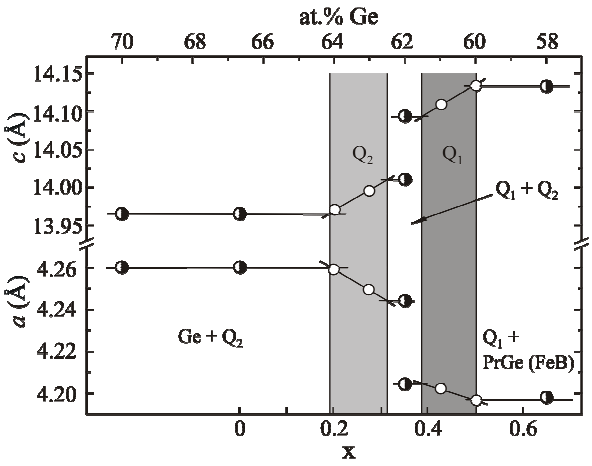

Fig. 2 Cell parameters corresponding to the α-$ThSi_2$ type and homogeneity ranges of the non-stoichiometric praseodymium digermanides Q_2 and Q_1.

Fractional atom coordinates and anisotropic displacement parameters for Pr_4Ge_7 (Pearson symbol *oS*44, space group $C222_1$) are presented in Table 4. The refinement showed no indication for the presence of Al in the structure or for any deviation from an ordered arrangement of vacancies. The positional parameters were standardized with the program STRUCTURE TIDY [21]. The anisotropic displacement parameters of sites Ge(3) and Ge(4) show relatively large values, the corresponding ellipsoids being elongated in the direction towards the vacant Ge site. The shortest interatomic distances, listed in Table 5, are in agreement with usual values observed for Pr-Pr, Pr-Ge, and Ge-Ge distances.

Fig. 3 shows a projection of the structure of Pr_4Ge_7, along the shortest translation vector, [100]. The translation unit *b* corresponds to the *c*-parameter of the parent structure α-$ThSi_2$. As in the parent structure, each Ge site is surrounded by six Pr atoms forming a trigonal prism. The prisms exhibit minor distortions, and the centering Ge atoms are displaced from the prism center, leading to Ge-Pr distances ranging from 3.06 to 3.63 Å in the case of site Ge(3).

The structure type α-$ThSi_2$ is characterized by a 3D-framework of Si-Si contact distances, where each Si atom is surrounded by three other Si atoms. Hexagons appear in the projection of the framework

formed by the majority element, shown in Fig. 4. The absence of 1/8 of the Ge atoms in Pr_4Ge_7 with respect to the α-$ThSi_2$ type causes interruptions in the framework, but the 3D-character of the Ge substructure is preserved. It can be seen from Fig. 4 that part of the hexagons present in the projection of the parent type remain. This is not the case in the related vacancy derivative Y_3Ge_5 (space group *Fdd*2), where 1/6 of the Ge positions are vacant. The list of interatomic distances in Table 5 confirms that the sites Ge(1) and Ge(2) in Pr_4Ge_7 have as nearest neighbors three other Ge atoms at distances 2.43-2.66 Å, whereas the sites Ge(3) and Ge(4) have only two Ge atoms at similar distances.

Table 6 groups several partly or fully ordered vacancy derivatives of α-$ThSi_2$. In all these structures the construction of fused trigonal prisms formed by the large atoms remains. The types are ordered according to increasing amount of empty prisms centers. No As-As contact distances exist in the structure type NbAs, where second *M* (As) position is vacant. An extended discussion about vacancy derivatives of α-$ThSi_2$ can be found in the works by Venturini *et al.* [12,15].

Table 3 Crystal data and details of the data collection and refinement for Pr_4Ge_7.

Nominal composition of the sample		$Pr_{33.3}Al_{6.7}Ge_{60}$
Mass per formula unit M_r		1071.8
Space group		$C222_1$ (#20)
Cell parameters	*a* (Å)	6.007(2)
	b (Å)	13.987(4)
	c (Å)	12.009(4)
Cell volume *V* (Å^3)		1009.0(4)
Formula units per unit cell *Z*		4
Density D_x (Mg·m^{-3})		7.055
Radiation, wavelength (Å)		Mo *Kα*, 0.71073
Temperature for data collection (K)		293
Crystal size (mm)		0.025×0.035×0.045
Crystal color		gray, metallic
Scan method		*ω*-2*θ*
Absorption correction		empirical (*ψ*-scans)
Transmission factors T_{min}-T_{max}		0.590-1.000
Number of measured reflections		2672
Number of independent reflections, R_{int}		651, 0.112
Limit for data collection θ_{max} (°)		30
Range of indexes	*h*	0→8
	k	-19→19
	l	0→16
Refinement on		*F*
Reliability factors	*R*	0.110
	wR	0.057
Number of refined parameters		54
Extinction coefficient		1.2(1)×10^{-4}

Table 4 Fractional atomic coordinates and anisotropic displacement parameters (Å^2) in the structure of Pr_4Ge_7 ($C222_1$, *a* = 6.007(2), *b* = 13.987(4), *c* = 12.009(4) Å).

Site	Wyckoff position	*x*	*y*	*z*	U_{11}	U_{22}	U_{33}	U_{12}	U_{13}	U_{23}
Pr(1)	8*c*	0.2377(6)	0.2461(1)	0.3782(1)	0.014(2)	0.004(1)	0.004(2)	-0.001(1)	-0.001(1)	-0.003(1)
Pr(2)	4*b*	0	0.5034(4)	¼	0.004(2)	0.008(1)	0.007(2)	0	-0.002(1)	0
Pr(3)	4*a*	0.0087(7)	0	0	0.004(2)	0.010(1)	0.007(2)	0	0	0.003(1)
Ge(1)	8*c*	0.016(1)	0.4135(3)	0.0105(5)	0.005(3)	0.005(2)	0.006(3)	-0.003(2)	0.005(3)	-0.002(2)
Ge(2)	8*c*	0.2513(7)	0.1721(3)	0.1272(3)	0.004(2)	0.015(2)	0.004(2)	-0.003(1)	0.001(2)	0.004(1)
Ge(3)	8*c*	0.313(1)	0.3493(4)	0.1567(6)	0.043(4)	0.027(3)	0.034(4)	0.025(3)	0.037(3)	0.024(3)
Ge(4)	4*b*	0	0.0642(5)	¼	0.013(3)	0.039(4)	0.015(4)	0	-0.003(4)	0

Table 5 Interatomic distances (Å) in the structure of Pr_4Ge_7.

Pr(1)	– 1 Ge(3)	3.060(6)	Pr(2)	– 2 Ge(3)	3.072(6)
	– 1 Ge(3)	3.089(7)		– 2 Ge(4)	3.122(3)
	– 1 Ge(1)	3.097(5)		– 2 Ge(1)	3.140(6)
	– 1 Ge(1)	3.114(6)		– 2 Ge(2)	3.158(5)
	– 1 Ge(2)	3.115(5)		– 2 Ge(1)	3.339(6)
	– 1 Ge(2)	3.188(5)		– 2 Pr(1)	4.047(3)
	– 1 Ge(2)	3.202(4)		– 2 Pr(1)	4.167(3)
	– 1 Ge(2)	3.240(6)		– 2 Pr(3)	4.210(3)
	– 1 Ge(4)	3.299(6)		– 2 Pr(3)	4.284(3)
	– 1 Ge(3)	3.614(6)			
	– 1 Ge(3)	3.634(7)	Pr(3)	– 2 Ge(3)	3.060(5)
	– 1 Pr(3)	4.022(3)		– 2 Ge(4)	3.134(2)
	– 1 Pr(2)	4.047(3)		– 2 Ge(1)	3.200(8)
	– 1 Pr(3)	4.132(3)		– 2 Ge(2)	3.203(4)
	– 1 Pr(2)	4.167(3)		– 2 Ge(1)	3.281(8)
	– 2 Pr(1)	4.194(4)		– 2 Pr(1)	4.022(3)
	– 1 Pr(1)	4.200(4)		– 2 Pr(1)	4.132(3)
	– 1 Pr(1)	4.406(4)		– 2 Pr(2)	4.210(3)
				– 2 Pr(2)	4.284(3)
Ge(1)	– 1 Ge(1)	2.433(9)			
	– 1 Ge(2)	2.588(8)	Ge(3)	– 1 Ge(2)	2.531(8)
	– 1 Ge(3)	2.659(9)		– 1 Ge(1)	2.659(9)
	– 1 Pr(1)	3.097(5)		– 1 Pr(1)	3.060(6)
	– 1 Pr(1)	3.114(6)		– 1 Pr(3)	3.060(5)
	– 1 Pr(2)	3.140(6)		– 1 Pr(2)	3.072(6)
	– 1 Pr(3)	3.200(8)		– 1 Pr(1)	3.089(7)
	– 1 Pr(3)	3.281(8)		– 1 Pr(1)	3.614(6)
	– 1 Pr(2)	3.339(6)		– 1 Pr(1)	3.634(7)
Ge(2)	– 1 Ge(3)	2.531(8)	Ge(4)	– 2 Ge(2)	2.569(6)
	– 1 Ge(4)	2.569(6)		– 2 Pr(2)	3.122(3)
	– 1 Ge(1)	2.588(8)		– 2 Pr(3)	3.134(2)
	– 1 Pr(1)	3.115(5)		– 2 Pr(1)	3.299(6)
	– 1 Pr(2)	3.158(5)			
	– 1 Pr(1)	3.188(5)			
	– 1 Pr(1)	3.202(4)			
	– 1 Pr(3)	3.203(4)			
	– 1 Pr(1)	3.240(6)			

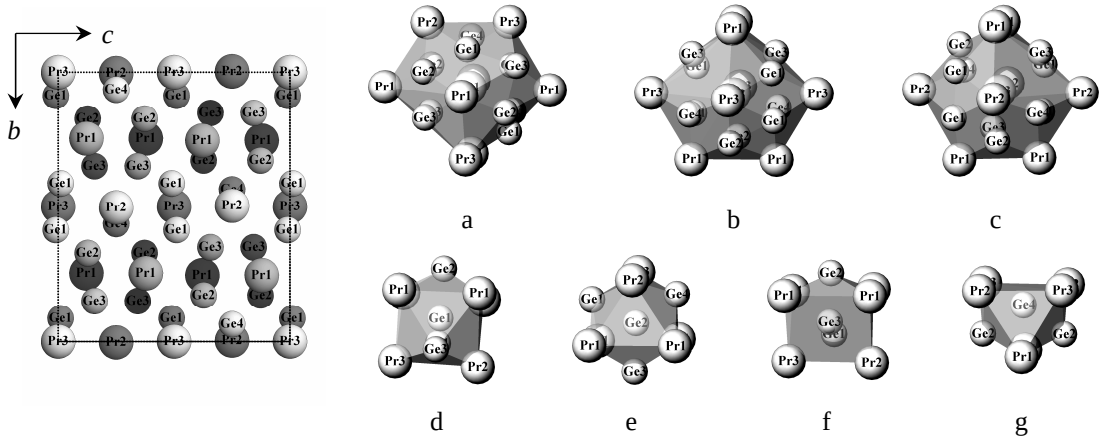

Fig. 3 Projection of the structure of Pr_4Ge_7 along [100] and coordination polyhedra: $Pr(1)Ge_{11}Pr_8$ (a), $Pr(2)Ge_{10}Pr_8$ (b), $Pr(3)Ge_{10}Pr_8$ (c), $Ge(1)Pr_6Ge_3$ (d), $Ge(2)Pr_6Ge_3$ (e), $Ge(3)Pr_6Ge_2$ (f), $Ge(4)Pr_6Ge_2$ (g).

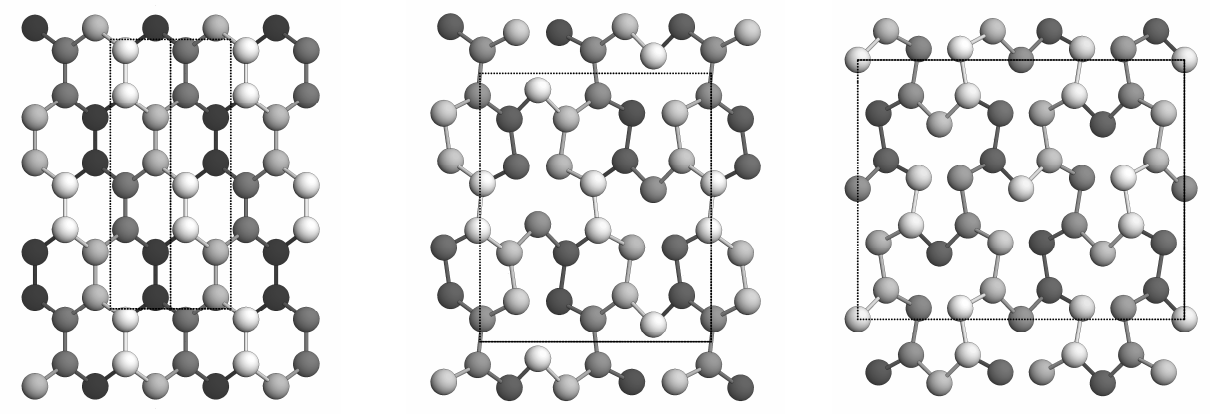

a b c

Fig. 4 Projections of the framework formed by the majority element in the structures of α-$ThSi_2$ (a), Pr_4Ge_7 (b) and Y_3Ge_5 (c).

Table 6 Simple vacancy derivatives RM_{2-x} of the α-$ThSi_2$ structure type.

x	Structure type	Space group	Pearson symbol	Translation vectors with respect to α-$ThSi_2$			Reference
0	α-$ThSi_2$	$I4_1/amd$	$tI12$	**a**	**b**	**c**	[22]
0.25	Nd_4Ge_7	$C222_1$	$oS44$	-**a** + **b**	**c**	2(**a** + **b**)	[12]
0.25	$ThNi_{1.75}$	$C2/c$	$mS12$-1	**a** + **b**	-**a** + **b**	(-**a** - **b** + **c**)/2	[23]
0.33	Y_3Ge_5	$Fdd2$	$oF64$	-**a** + **b**	3(**a** + **b**)	**c**	[14]
0.39	$CeGe_{0.66}Si_{0.95}$	$I\bar{4}m2$ [a]	$tI12$-1.56	**a**	**b**	**c**	[24]
0.44	Ce_9Ge_{14}	$I4_1$	$tI104$-12	3**a**	3**b**	**c**	[25]
0.60	α-$GdSi_{1.4}$	$Imma$	$oI12$-2.4	**a**	**b**	**c**	[26]
1	NbAs	$I4_1md$	$tI8$	**a**	**b**	**c**	[27]

[a] originally reported in space group $F222$ (see [4])

References

[1] I.O. Nasibov, P.G. Rustamov, M.M. Aliyeva, *Russ. Metall.* (5) (1973) 163-167.

[2] V.N. Eremenko, Xuong Quok Che, Yu.I. Buyanov, A.M. Khar'kova, *Inorg. Mater.* 11 (1975) 133-135.

[3] A.B. Gokhale, A. Munitz, G.J. Abbaschian, *Bull. Alloy Phase Diagrams* 10 (1989) 241-246.

[4] P. Villars, K. Cenzual (Eds.), *Pearson's Crystal Data, Crystal Structure Database for Inorganic Compounds*, ASM International, Materials Park (OH), 2007.

[5] I.A. Gryniv, V.K. Pecharsky, Ya.P. Yarmolyuk, O.I. Bodak, V.A. Bruskov, *Sov. Phys. Crystallogr.* 32 (1987) 460-461.

[6] N.Z. Nakonechna, I.A. Savysyuk, *Visn. Lviv. Univ. Ser. Khim.* 38 (1999) 21-25.

[7] H.F. Yang, G.H. Rao, W.G. Chu, G.Y. Liu, Z.W. Ouyang, J.K. Liang, *J. Alloys Compd.* 339 (2002) 189-194.

[8] P. Schobinger Papamantellos, K.H.J. Buschow, *J. Less-Common Met.* 111 (1985) 125-138.

[9] P. Schobinger-Papamantellos, D.B. de Mooij, K.H.J Buschow, *J. Magn. Magn. Mater.* 89 (1990) 47-55.

[10] B. Lambert-Andron, J. Pierre, B. Chenevier, R. Madar, N. Boutarek, J. Rodriguez-Carvajal, *J. Phys.: Condens. Matter* 6 (1994) 8725-8732.

[11] N. Boutarek, J. Pierre, B. Lambert-Andron, Ph. L'Heritier, R. Madar, *J. Alloys Compd.* 204 (1994) 251-260.

[12] G. Venturini, I. Ijjaali, B. Malaman, *J. Alloys Compd.* 289 (1999) 168-177.

[13] R.E. Gladyshevskii, I.A. Savysyuk, K. Cenzual, *Coll. Abstr. 6 Int. School-Conf. "Phase Diagrams in Materials Science"*, Kiev, 2001, p. 20.

[14] V.A. Bruskov, O.I. Bodak, V.K. Pecharskii, E.I. Gladyshevskii, L.O. Muratova, *Sov. Phys. Crystallogr.* 28 (1983) 151-153.

[15] G. Venturini, I. Ijjaali, B. Malaman, *J. Alloys Compd.* 285 (1999) 194-203.

[16] I.A. Savysyuk, *Thesis*, Ivan Franko National University of Lviv, 2000.

[17] N.Z. Semuso, *Thesis*, Ivan Franko National University of Lviv, 2002.

[18] W. Kraus, G. Nolze, *PowderCell for Windows*, Federal Institute for Materials Research and Testing, Berlin, 1999.

[19] D. Schwarzenbach, *Program LATCON: Refine Lattice Parameters*, University of Lausanne, 1966.

[20] G.M. Sheldrick, *SHELXL. Release 97-1*, University of Göttingen, 1997.
[21] L.M. Gelato, E. Parthé, *J. Appl. Crystallogr*. 20 (1987) 139-143.
[22] G. Brauer, A. Mitius, *Z. Anorg. Allg. Chem.* 249 (1942) 325-339.
[23] A. Palenzona, S. Cirafici, *J. Less-Common Met.* 142 (1988) 311-317.
[24] N. Boutarek, R. Madar, B. Lambert Andron, S. Auffret, J. Pierre, *J. Alloys Compd.* 189 (1992) 9-15.
[25] B. Lambert-Andron, E. Houssay, R. Madar, F. Hippert, J. Pierre, S. Auffert, *J. Less-Common Met.* 167 (1990) 53-63.
[26] J.A. Perri, I. Binder, B. Post, *J. Phys. Chem.* 63 (1959) 616-619.
[27] H. Boller, E. Parthé, *Acta Crystallogr.* 16 (1963) 1095-1101.